Nonlinear optical absorption of Ti_3C_2 quantum dots regulated by Ag nanoparticles

JIA LIU[1], YABIN SHAO[2], SHIYI ZUO[1], YACHEN GAO[1,*]
[1]*Electronic Engineering College, Heilongjiang University, Harbin, 150080, China*
[2]*School of Jia Yang, Zhejiang Shuren University, Shaoxing, 312028, China*

The nonlinear absorption of Ti_3C_2 quantum dots (QDs), Ag nanoparticles and Ti_3C_2 QDs-Ag nanocomposites were studied by using nanosecond Z-scan technique. It was found that, Ti_3C_2 QDs and Ag nanoparticles exhibit saturation absorption (SA), while the Ti_3C_2 QDs-Ag nanocomposites can exhibit SA or reverse saturation absorption (RSA) depending laser intensity. The investigation indicates that adding of Ag nanoparticles can regulate the nonlinear absorption of Ti_3C_2 QDs, even make it change from SA to RSA. The origin of nonlinear absorption and transformation was also analyzed and discussed in terms of plasmon bleaching.

(Received January 5, 2022; accepted June 6, 2022)

Keywords: Ti_3C_2 quantum dots, Ti_3C_2 QDs-Ag nanocomposites, Nonlinear absorption, Z-scan

1. Introduction

With the rapid development of the optoelectronic equipment industry, two-dimension (2D) nanomaterials have attracted extensive attention and great research interest due to their excellent in-plane transmission characteristics [1]. Graphene nanosheets (GNs) are the initial two-dimensional nanomaterials which have been extensively studied from synthesis to application [2]. Further research on graphene has led to developing other new two-dimension single-element nanosheets, such as silylene, and phosphazene [3]. However, because they are quite difficult to prepare on a large scale, and their stability faces major challenges. Therefore, relatively stable two-element nanosheets have been explored and used in practical applications [4]. Among them, 2D MXenes (consisting of transition metal carbides, nitrides or carbonitrides with a thickness of several atomic layers) [5], due to their excellent photoelectric performance, have attracted more and more attention from professionals in the fields of dielectric, photovoltaic, luminescence, battery devices, and capacitors [6].

In recent years, quantum dots prepared from 2D materials have also received widespread attention, such as graphene quantum dots (GQDs), carbon dots (CDs), polymer dots [7], and black phosphorus (BP) dots [8]. They have become excellent fluorophores for bio-imaging and optical sensing due to their unique nature including adjustable photoluminescence (PL), good water solubility, molecular size, excellent optical stability, chemical inertness, easy to internalize cells, biocompatibility, low cost, and easily functionalized. Enlightened by the uniqueness of GQDs and BP dots [9-11], people have invested a lot of time and energy to explore other quantum dots based on new 2D materials such as Ti_3C_2 QDs. Some research has been devoted to their synthesis, luminescence properties and intracellular fluorescent labeling of Ti_3C_2 QDs. In 2017, Zhi Chunyi et al. studied the chemical structure and luminescence mechanism of Ti_3C_2 QDs prepared for the first time. The obtained Ti_3C_2 QDs have excellent blue luminescence, and the PL quantum yield is up to 10% [12]. In 2019, Qihuang Deng et al. used solvent-aided sonication to strip the original MXene to obtain the few-layer of MXene. The amine-assisted solvothermal method was used to cut the few-layer MXene into the small-size nitrogen-doped MXene quantum dots [13]. In 2019, Xiumei Xu et al. found that Ti_3C_2 QDs can present bright blue light emission under ultraviolet excitation. So they designed an intracellular glutathione (GSH) flourescence sensor based on the Ti_3C_2 QDs [14].

In fact, nonlinear optical properties of Ti_3C_2 QDs are also very important for their applications in photo-electronic devices. But up to now, relatively less investigation has been conducted on their optical nonlinearities. In 2020, Shixiang Xu et al. used femtosecond open aperture Z-scan experiments to investigate the nonlinear absorption of Ti_3C_2 QDs at wavelengths of 540, 800, 1060 and 1550 nm respectively [15]. They found that Ti_3C_2 QDs showed saturated absorption characteristics under different wavelength excitation. In order to gain a deeper understanding of the nonlinear absorption process of Ti_3C_2 QDs, in this paper, open aperture (OA) Z-scan is executed at the different excitation wavelengths and energies.

2. Samples and experiments

Ti_3C_2 QDs was synthesized by using the method reported in the reference [16]. Firstly, the aluminum layer in Ti_3AlC_2 is selectively etched with hydrofluoric acid to obtain bulk Ti_3C_2 MXene. Then by solvothermal method using oleylamine as surface passivator Ti_3C_2 QDs were obtained from Ti_3C_2 MXene. Silver nanoparticles was synthesized using the reduction of $AgNO_3$ [17]. Firstly, 36 mg $AgNO_3$ was dissolved in 200 ml deionized water under constant magnetic stirring and heated to boiling. Then 4 ml 1wt% sodium citrate solution was added into the $AgNO_3$ solution and boiled for about 30 minutes until the solution turns brown and fluoresces green. Finally, silver nano-colloids were obtained. Ti_3C_2 QDs and Ag nano-colloids with the same transmittance were mixed in equal proportions and subjected to water bath ultrasonic treatment to obtain Ti_3C_2 QDs-Ag nanocomposites. The Ti_3C_2 QDs and Ti_3C_2 QDs-Ag nanocomposites were characterized by Transmission Electron Microscope (TEM). Subsequently, linear absorption was measured using a UV-visible spectrophotometer (TU-1901, Beijing Purkinje General Instrument Co., Ltd).

Nonlinear absorption was studied via typical OA Z-scan experiment [18]. The schematic diagram of the experimental setup is shown in Fig. 1. A 6 ns 10 Hz Q-switched Nd:YAG laser (Surelite II, Continuum, Santa Clara, CA, USA) and an optical parametric oscillator (APE OPO, Continuum) were used as excitation source. A lens with a focal length of 20 cm is used to focus laser beam on a quartz cuvette (2 mm) containing the sample. And the focus spot size is about 100 μm. During experiments, two laser energy meters (EPM 2000, Coherent) are used to measure the incident and transmitted laser energy. The energies are recorded by a computer.

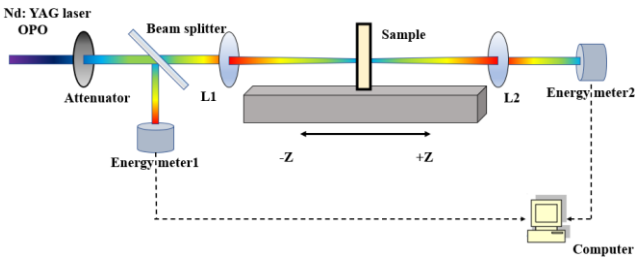

Fig. 1. Schematic diagram of the OA Z-scan experimental setup (color online)

3. Results and discussions

Figs. 2(a) and (b) present the TEM images of the Ti_3C_2 QDs and Ti_3C_2 QDs-Ag nanocomposites, respectively. Fig. 2(a) reveals that the shape of the Ti_3C_2 QDs is about sphere, and the size is about 20 nm. The Ti_3C_2 QDs-Ag nanocomposites are shown in Fig. 2(b), in which the grey ones are Ti_3C_2 QDs, the black dots are Ag nanoparticles with the size of about 20 nm.

The absorption spectra of Ti_3C_2 QDs, Ag nanoparticles and Ti_3C_2 QDs-Ag nanocomposites are shown in Figs. 3(a), (b) and (c), respectively.

It can be found from Fig. 3(a) that there is a weak absorption peak at about 750 nm, which may be caused by its intra-band transition [19]. In Fig. 3(b), we find an absorption peak at about 410 nm which is owing to the surface plasmon resonance (SPR) in Ag nanoparticles [20]. Fig. 3(c) shows the absorption spectra of Ti_3C_2 QDs-Ag nanocomposites. The spectra is almost same as one in Fig. 3(a). Besides, there is an enhanced peak around 410 nm originating from SPR.

The nonlinear absorption of the Ti_3C_2 QDs, Ag nanoparticles and Ti_3C_2 QDs-Ag nanocomposites were studied by the traditional OA Z-scan conducted under 500, 532 and 550 nm laser pulses from an OPO. The experimental results at three different energies of 750, 1080 and 1380 μJ are shown in Fig. 4.

Fig. 4(a) shows the experimental results under 500 nm laser pulse for 750 μJ energy. For the Ti_3C_2 QDs and Ag nanoparticles, strong SA is observed. However, for the Ti_3C_2 QDs-Ag nanocomposites, when the sample moved to the beam focus, the transmission increases, but as the sample gradually moves away from the focus the transmittance of the specimen decreases, which means that the transition from SA to RSA. In Figs. 4(b) and (c), the results have the same trend as that in Fig. 4(a), but it is evident that the amplitude of SA of Ti_3C_2 QDs and Ag nanoparticles increases with excitation energy. The RSA in Ti_3C_2 QDs-Ag nanocomposites is becoming more and more obvious. From Figs. 4(a), (d), and (g), we can see the results at different wavelengths under the excitation energy at 750 μJ. For the Ag nanoparticles, as the excitation wavelength becomes longer, the SA becomes weaker. The reason is that the absorption peak of Ag nanoparticles is around 410 nm, when the excitation wavelength becomes longer, it is farther away from its resonance region. For the Ti_3C_2 QDs, the changing of wavelength used in the experiment has little effect on nonlinear absorption. For Ti_3C_2 QDs-Ag nanocomposites, the RSA gradually decreases with the increase of wavelength, but at 550 nm, the composite material does not appear RSA. The reason may be that the excitation energy is low and the Ag nanoparticles involved in the regulation are in the non-resonant region at 550nm. However, in Figs. 4(h) and (i), we can clearly see that the Ti_3C_2 QDs-Ag nanocomposites have RSA. Moreover, the RSA intensity also deepens with the increase of excitation energy. This is because a higher excitation energy can excite the ground state or excited state particles to jump to a higher energy level, resulting in the phenomenon of RSA. In general, the RSA is related to two photon absorption [21].

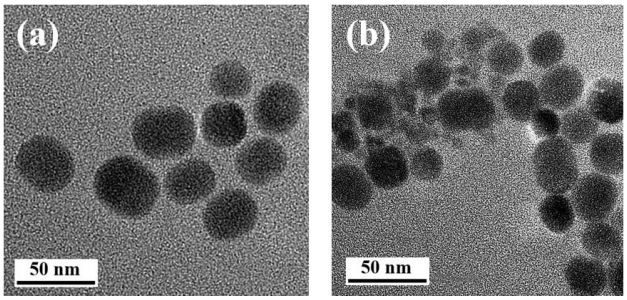

Fig. 2. The TEM images of the (a) Ti_3C_2 QDs, (b) Ti_3C_2 QDs-Ag nanocomposites (color online)

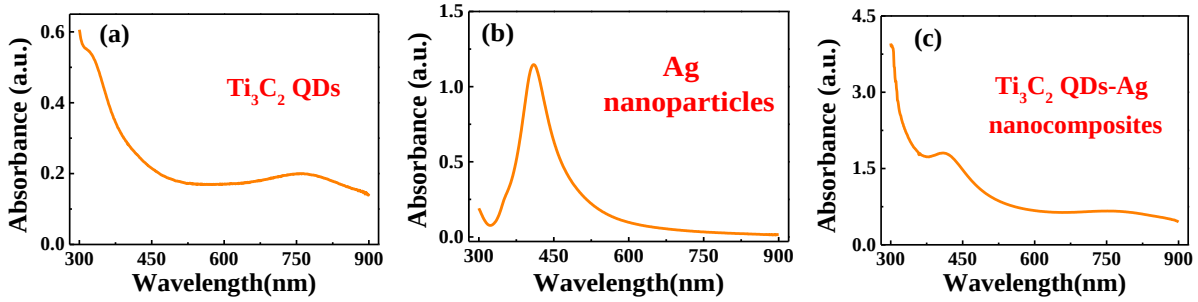

Fig. 3. UV-vis-NIR absorption spectra for the (a) Ti_3C_2 QDs, (b) Ag nanoparticles and (c) Ti_3C_2 QDs-Ag nanocomposites (color online)

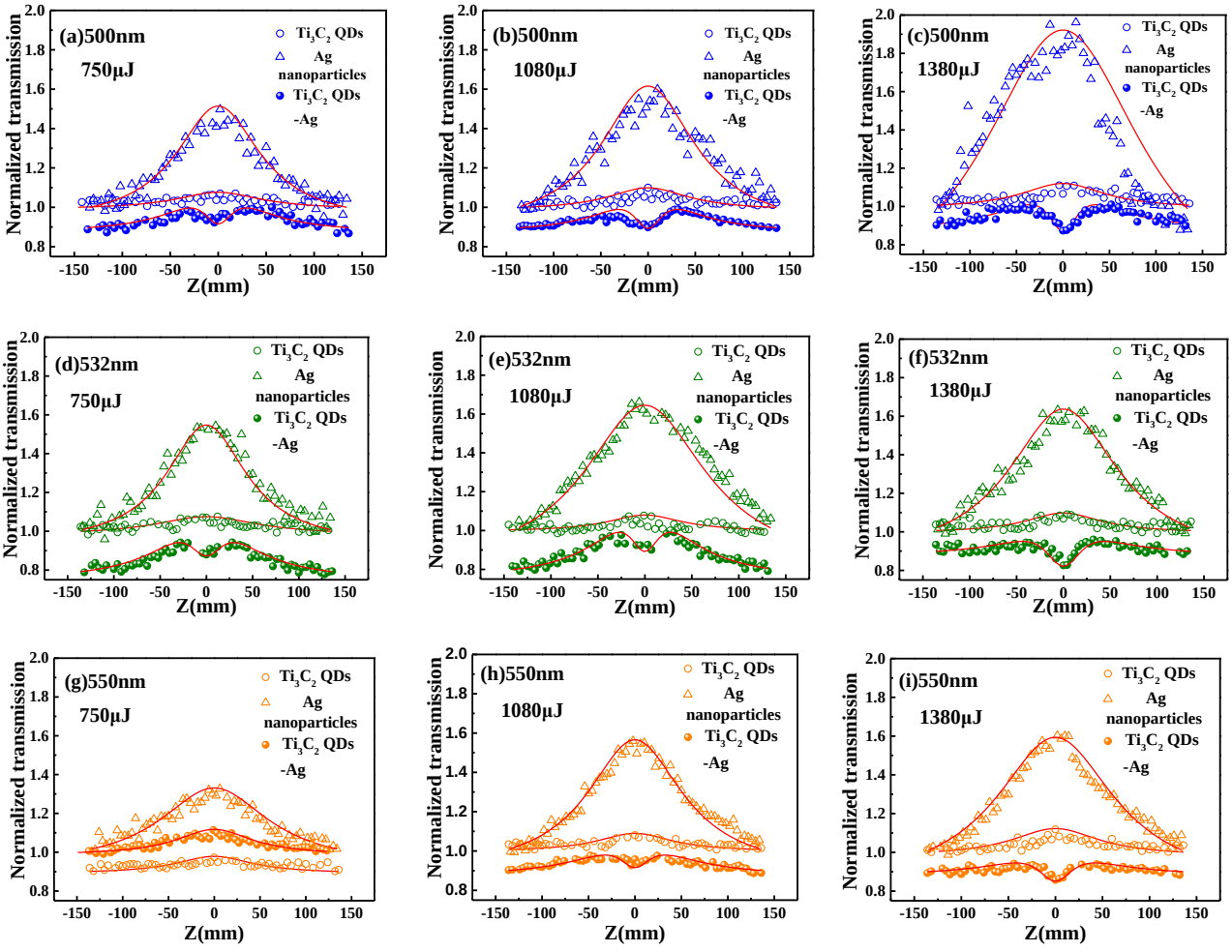

Fig. 4. Normalized transmission of Ti_3C_2 QDs, Ag nanoparticles and Ti_3C_2 QDs-Ag nanocomposites for OA Z-scan at disparate energies and wavelengths (a-c) 500 nm, (d-f) 532 nm, (g-i) 550 nm, and the solid curves are the theoretical fitting (color online)

It can be seen from the results of above that there are two kinds of nonlinear absorption with inverse sign in samples. To analyze the conversion from SA to RSA, the following expression of absorption coefficient $\alpha(I)$ can be used [18]:

$$\alpha(I) = \frac{\alpha_0}{1+(I/I_s)} + \beta I \quad (1)$$

where α_0 is the linear absorption coefficient, I_s is saturation intensity, I is incident laser intensity, β is two photon absorption coefficient.

We know that the incident laser intensity can be expressed as:

$$I = \frac{I_0}{1+z^2/z_0^2} \quad (2)$$

Therefore, Eqs. (1) can be further expressed as:

$$\alpha(I_0) = \frac{\alpha_0}{1+\frac{I_0}{(1+z^2/z_0^2)I_s}} + \frac{\beta I_0}{1+z^2/z_0^2} \quad (3)$$

Theoretically, when only two-photon absorption occurs, the OA Z-scan transmittance normalization data can be expressed as [22]:

$$T(z) = \sum_{m=0}^{\infty} \frac{[-q_0(z)]^m}{(m+1)^{3/2}} \approx 1 - \frac{\beta I_0 L_{eff}}{2\sqrt{2}\left(1+\frac{z^2}{z_0^2}\right)} \quad (4)$$

where I_0 is the peak intensity on-axis at the focus, $q_0(z) = \beta I_0 L_{eff}/(1+z^2/z_0^2)$, $L_{eff} = (1-e^{-\alpha_0 L})/\alpha_0$, L_{eff} is the resultful coactions length, z is the lengthways shift of the sample from the focusing position ($z=0$), L is the sample thickness, z_0 is Rayleigh diffraction range, m is the whole number from 0 to m. When the β is small, the first order approximation of Eqs. (4) is as follows:

$$\beta = 2\sqrt{2}[1-T(z=0)](1+z^2/z_0^2)/I_0 L_{eff} \quad (5)$$

According to Eqs. (1)-(5), the I_0, I_s and β can be gained by fitting the data and their values are shown in Table 1.

Table 1. Nonlinear optical parameters of the Ti_3C_2 QDs, Ag nanoparticles and Ti_3C_2 QDs-Ag nanocomposites

λ(nm)	$E(\mu J)$	I_0 (MW/cm^2)	I_s (10^{-2}MW/cm^2) (Ti_3C_2 QDs)	I_s (10^{-2}MW/cm^2) (Ag nanoparticles)	I_s (10^{-2}MW/cm^2) (Ti_3C_2 QDs-Ag)	β(10^{-9}cm/mW) (Ti_3C_2 QDs-Ag)
500	750	0.299	0.368	0.232	0.489	0.921
500	1080	0.431	0.590	0.334	0.726	0.873
500	1380	0.551	0.737	0.382	0.754	0.980
532	750	0.299	0.387	0.168	0.483	1.254
532	1080	0.431	0.458	0.349	0.719	1.196
532	1380	0.551	0.664	0.353	0.754	1.227
550	750	0.299	0.405	0.180	0.457	-
550	1080	0.431	0.551	0.275	0.696	0.658
550	1380	0.551	0.728	0.370	0.755	0.713

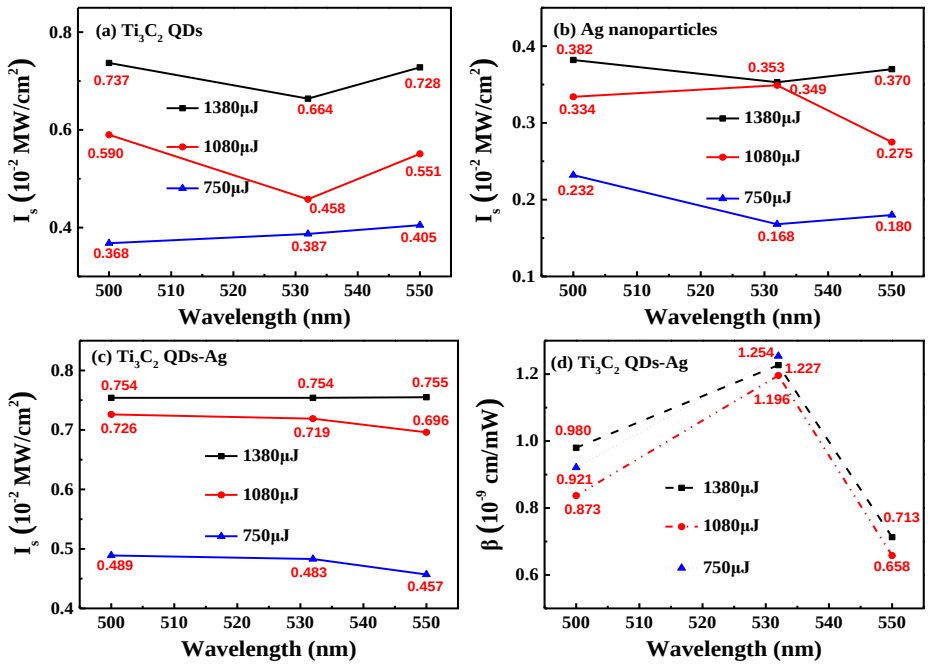

Fig. 5. The dots are relationship between (a) Ti_3C_2 QDs, (b) Ag nanoparticles I_s and wavelength at different energies. The relationship between (c) I_s and (d) β of Ti_3C_2 QDs-Ag nanocomposites versus the wavelength of different energy (color online)

In order to observe the dependence of nonlinear absorption on wavelength, the I_s and β changing with wavelength are shown in Figs. 5(a)-(d).

It can be seen from Figs. 5(a) and (b) that when the excitation wavelength is close to the linear absorption peak, the I_s of Ti_3C_2 QDs and Ag nanoparticles increases. When the irradiance is moderate, the bleaching of the ground state plasma band leads to the generation of SA [23]. When the excitation wavelength is close to the SPR peak of Ti_3C_2 QDs-Ag nanocomposites, as shown in Fig. 5(c), the I_s increases accordingly; in Fig. 5(d), the β decreases. The reason for this phenomenon is that when excitation wavelength is close to the SPR the I_s increases of Ti_3C_2 QDs-Ag nanocomposites. The β decreases because more electrons are pumped to the conduction band and the absorption of free carriers is enhanced.

4. Conclusion

We studied the nonlinear absorption of Ti_3C_2 QDs, Ag nanoparticles and Ti_3C_2 QDs-Ag nanocomposites using OA Z-scan measurements. The results show that the addition of Ag nanoparticles can adjust the nonlinear absorption of Ti_3C_2 QDs, even cause the conversion from SA to RSA of Ti_3C_2 QDs. We think that the transformation results from the competition of ground state plasma beaching two photon absorption. Correspondingly, some optical parameters were obtained. The strategy proposed here may be used in the design of new optoelectronic devices.

Acknowledgement

This work was supported by the East University of Heilongjiang Scientific Research Fund (HDFHX210110, 210111, HDFKYTD202105), Natural Science Foundation of Heilongjiang Province (LH2021A019) and Scientific research fund of Zhejiang Shuren University (2021R037).

References

[1] L. Yan, T. Bo, P.-F. Liu, B.-T. Wang, Y.-G. Xiao, M.-H. Tang, Journal of Materials Chemistry C **9**(7), 2589 (2019).
[2] S. J. Guo, S. J. Dong, Chemical Society Reviews **5**(40), 2644 (2011).
[3] D. M. Salazar, A. K. Gupta, A. Orthaber, Dalton Transactions **31**(47), 10404 (2018).
[4] Y. Shu, W. Zhang, H. Cai, Y. Yang, X. Yu, Q. Gao, Nanoscale **14**(11), 6644 (2019).
[5] M. W. Barsoum, Progress in Solid State Chemistry **1**(28), 201 (2000).
[6] M. Li, J. Lu, K. Luo, Y. Li, K. Chang, K. Chen, J. Zhou, J. Rosen, L. Hultman, P. Eklund, P. O. A. Persson, S. Du, Z. Chai, Z. Huang, Q. Huang, Journal of the American Chemical Society **11**(141), 4730 (2019).
[7] K. A. Ritter, J. W. Lyding, Nature Materials **3**(8), 235 (2009).
[8] P. F. Chen, N. Li, X. Z. Chen, W. J. Ong, X. J. Zhao, 2d Materials **5**, 014002 (2018).
[9] J. Wurm, A. Rycerz, N. Adagideli, M. Wimmer, K. Richter, H. U. Baranger, Physical Review Letters **5**(102), 056806 (2008).
[10] X. Zhang, H. Xie, Z. Liu, C. Tan, Z. Luo, H. Li, J. Lin, L. Sun, W. Chen, Z. Xu, Angewandte Chemie International Edition **12**(54), 3653 (2015).
[11] B. C. M. Martindale, G. A. M. Hutton, C. A. Caputo, S. Prantl, R. Godin, J. R. Durrant, E. Reisner, Angewandte Chemie-International Edition **23**(56), 6459 (2017).
[12] Q. Xue, H. J. Zhang, M. S. Zhu, Z. X. Pei, H. F. Li, Z. F. Wang, Y. Huang, Y. Huang, Q. H. Deng, J. Zhou, S. Y. Du, Q. Huang, C. Y. Zhi, Advanced Materials **15**(29), 1604847 (2017).
[13] Y. Feng, F. Zhou, Q. Deng, C. Peng, Ceramics International **6**(46), 8320 (2020).
[14] X. Xu, H. Zhang, Q. Diao, Y. Zhu, G. Yang, B. Ma, Journal of Materials Science-Materials in Electronics **1**(31), 175 (2020).
[15] F. Yang, Y. Ge, T. Yin, J. Guo, F. Zhang, X. Tang, M. Qiu, W. Liang, N. Xu, C. Wang, ACS Applied Nano Materials **12**(3), 11850 (2020).
[16] S. Y. Lu, L. Z. Sui, Y. Liu, X. Yong, G. J. Xiao, K. J. Yuan, Z. Y. Liu, B. Z. Liu, B. Zou, B. Yang, Advanced Science **9**(6), 1801470 (2019).
[17] B. Palpant, Chapter: Third-Order Nonlinear Optical Response of Metal Nanoparticles, book: Non-Linear Optical Properties of Matter, Editors: Manthos G. Papadoupoulos, Andrezej J. Sadlej, Jerzy Leszczynski, Springer 461 (2006).
[18] M. Sheik-Bahae, A. A. Said, T. H. Wei, IEEE Journal of Quantum Electronics **4**(26), 760 (1990).
[19] H. Lashgari, M. R. Abolhassani, A. Boochani, S. M. Elahi, J. Khodadadi, Solid State Communications **195**, 61 (2014).
[20] Q. Chen, Y. Ye, J. Liu, S. Wu, P. Li, C. Liang, Journal of Colloid and Interface Science **585**, 444 (2021).
[21] A. S. Reyna, I. Russier-Antoine, F. Bertorelle, E. Benichou, P. Dugourd, R. Antoine, P.-F. Brevet, C. B. de Araújo, The Journal of Physical Chemistry C **32**(122), 18682 (2018).
[22] C. Pradeep, S. Mathew, B. Nithyaja, P. Radhakrishnan, V. P. N. Nampoori, Applied Physics a-Materials Science & Processing **1**(115), 291 (2014).
[23] J. T. Seo, Q. Yang, W.-J. Kim, J. Heo, S.-M. Ma, J. Austin, W. S. Yon, S. S. Jung, S. W. Han, B. Tabibi, D. Temple, Optics Letters **3**(34), 307 (2009).

*Corresponding author: gaoyachen@hlju.edu.cn